COMPARING ^{10}Be, IN SITU ^{10}Be, AND NATIVE ^{9}Be ACROSS A DIVERSE SET OF WATERSHEDS

A Thesis Progress Report Presented

by

Emily Sophie Greene

to

The Faculty of the Department of Geology

of

The University of Vermont

Dec 3rd, 2015

Submitted to the Faculty of the Geology Department, the University of Vermont, in partial fulfillment of the requirements for the degree of Master of Science specializing in Geology.

_____ (Advisor)

Paul Bierman, PhD

_____

Nicolas Perdrial, PhD

_____ (Chair)

Giuseppe A. Petrucci, PhD

1.0 Introduction

1.1 Background

Beryllium-10 (^{10}Be) is a cosmogenic radionuclide formed from the interaction of secondary cosmic rays with O, Mg, Si or Fe (Lal 1988). The vast majority of cosmic rays that react to produce ^{10}Be do so in the atmosphere, where ^{10}Be adheres to aerosols and is transported to surfaces via wet and dry deposition (Monaghan et al. 1986). This ^{10}Be is termed "meteoric" ($^{10}Be_{met}$). A small portion of cosmic radiation passes through the atmosphere to form "in situ" ^{10}Be ($^{10}Be_{is}$) in minerals on earth's surface (Bierman 1994). Unlike the $^{10}Be_{met}$ that is adsorbed to soils and sediment grains via relatively weak surface interactions, $^{10}Be_{is}$ is produced and thus trapped within a crystal lattice. $^{10}Be_{is}$ and $^{10}Be_{met}$ atoms accumulate in materials at or near the earth's surface, potentially making them a useful tracer of sediment movement and basin scale erosion rates (Pavich et al. 1984, Graly et al. 2010). While $^{10}Be_{is}$ has been used around the globe to measure millennial scale erosion rates, the potential for remobilization of $^{10}Be_{met}$ makes it difficult to interpret $^{10}Be_{met}$ data in terms of surface erosion rates (Portenga and Bierman 2011, Bacon et al. 2012).

Some (Barg et al. 1997, von Blanckenburg et al. 2012, Bacon et al. 2012) hypothesize that ^{9}Be that has weathered out of bedrock ($^{9}Be_{reactive}$) is likely to mirror the reactivity of $^{10}Be_{met}$ and can be used to help interpret $^{10}Be_{met}$ data in erosion rate studies. This hypothesis assumes that Be does not fractionate as it is weathered and transported with fluvial sediments. Using a mass balance approach, von Blanckenburg et al. (2012) propose a formula that calculates $^{10}Be_{met}/^{9}Be_{reactive}$-derived erosion rates. The purpose of my MS project is to better understand $^{10}Be_{met}$, ^{9}Be, and $^{10}Be_{is}$ dynamics and $^{10}Be_{met}/^{9}Be_{reactive}$-derived erosion rates by measuring $^{9}Be_{reactive}$ concentrations in over 200 fluvial sediment samples. This project is possible because I have access to fluvial sediment samples that others have collected from watersheds around the globe with diverse climactic, tectonic, and chemical environments (table 1) and analyzed for $^{10}Be_{met}$ and $^{10}Be_{is}$ concentrations.

While several methods of selectively extracting $^{9}Be_{raeactive}$ have been used in comparing $^{9}Be_{reactive}$ to $^{10}Be_{met}$ (Barg et al. 1997, Bacon et al. 2012, Wittmann et al. 2012), I hope to develop a method of extracting $^{9}Be_{reactive}$ that removes all ^{9}Be in grain coatings that can be applied to many types of samples such as fluvial sediments, lake sediments, or soils.

1.3 Hypotheses

My research aims at testing the following hypotheses.

1. The reactive phase of ^{9}Be can be effectively and consistently leached from grain coatings.
2. Fluvial sediment samples from a diverse set of watersheds display statistically significant relationships between $^{10}Be_{met}$, $^{10}Be_{is}$, and $^{9}Be_{reactive}$, and a range of watershed characteristics such as elevation, slope, relief, and mean annual precipitation.
3. $^{10}Be_{met}/^{9}Be_{reactive}$ -derived erosion rates calculated by the von Blanckenburg et al. (2012) mass balance formulation significantly correlate to $^{10}Be_{is}$-derived erosion rates in our dataset.

In order to test these hypotheses, I developed a method of $^{9}Be_{reactive}$ extraction, used that method to extract and analyze ^{9}Be concentrations from over 200 fluvial sediment samples, collected the relevant climatic and topographic data about the samples using ArcGIS, and performed statistical analyses of my results.

2.0 Work completed

2.1 Lab work

After examining the literature, I determined that leaching samples with HCl would selectively strip grain coatings (Barg et al. 1997, Bacon et al. 2012, Wittmann et al. 2012). First I performed a series of HCl leaching experiments in order to estimate the range of elemental concentrations I could expect from various samples. A small subset of samples was extracted for 24

hours in 6M HCL and the leachates were analyzed for Be, Ca, Mg, Si, Ti, Fe, Al, Mn, K, and Na using a JY Horiba Optima Ion Coupled Plasma-Optical Emission Spectrometer (ICP-OES). This preliminary leaching step allowed me to estimate the composition of leachate and determine the optimal range of standards for each element. Using these standard ranges, I developed a method that optimized the sensitivity of the ICP-OES for ppb detection of Be and ensured that overlapping emission peaks did not influence ^{9}Be concentrations (appendix 1). After measuring the concentrations of multi-element standards made to approximate concentrations of elements in leachates, I was confident that my method on the ICP-OES could accurately and precisely detect Be in leachates. I performed a series of HCl leach experiments on 3 samples: a soil sample (CPA-12), a fluvial sediment sample (QLD-5), and a glacial lake sediment sample (homogenized varve sample). The 3 samples (0.25 g each) were leached with 2 mL of 3M or 6M HCl in an ultrasonic bath for 1, 3, 8, or 24 hours. Samples were gravimetrically diluted, centrifuged, and the supernatants were analyzed using the optimized method on the ICP-OES. The results of this experiment showed that concentrations of ^{9}Be plateaued after 24 hours of reaction time in an ultrasonic bath (figure 1). I concluded that leaching sediments with 6M HCl in an ultrasonic bath for 24 hours extracted the entire grain coating for all sample types.

Once I had developed a method for leaching ^{9}Be from grain coatings, I extracted $^{9}Be_{reactive}$ from my fluvial sediment samples. In every batch of 50 samples, I processed 3 blank samples (same extraction procedure, but no sample is added), and 3 samples of homogenized varve sediment as a quality control. I also ran duplicates of 19 samples. These quality control measures allowed me to assess if my method of extraction was reproducible across batches. In addition to the 202 fluvial sediment samples used in my study, I also characterized the $^{9}Be_{reactive}$ and major element concentrations of leached grain coatings in over 200 fluvial sediment samples, glacial lake sediments samples, and soil samples for collaborators.

2.2 GIS analysis

Digital elevation models (DEM) for all watersheds were downloaded from the void-filled 3 arc-second STRM dataset (http://www2.jpl.nasa.gov/srtm/). Mean annual precipitation (MAP) data were downloaded from worldclim.org, a site that allows downloads from a global dataset of interpolated high-resolution monthly precipitation data. For all study areas except one (the Barron River), collaborators sent GIS-rendered watershed shapefiles that were used for analysis of ^{10}Be data (Trodick 2011). Using these shapefiles ensured that delineations of the watersheds were consistent across studies. Collaborators also provided $^{10}Be_{is}$-derived erosion rates that were calculated using the CRONUS algorithm (Balco et al. 2008). Watersheds corresponding to Barron River samples were delineated in ArcGIS using the hydrology toolset. Derived watershed characteristics matched the published data except for the watersheds of samples 1, 2, and 11 (Nichols et al. 2014), which matched the shapes and locations of published watershed figures, but did not match the calculated watershed area statistics. Mean elevation, total relief, mean slope, mean MAP, and mean latitude were calculated for each delineated watershed based on the global DEM and MAP datasets using zonal statistics.

2.3 Statistical analysis

Processing of data collected from HCl extraction experiments and GIS analysis was performed using the R programing language. Linear regression modeling allowed me to calculate the R^2 and p values for the correlations between $^{9}Be_{reactive}$, $^{10}Be_{met}$, $^{10}Be_{is}$, $^{10}Be_{is}$-derived erosion rates, mean annual precipitation, mean elevation, mean latitude, mean basin slope, total basin relief, and total basin area. I determined R^2 and p values associated with the correlations for each study area as well as across all sampling locations and produced plots to visualize the regressions. Finally, I replicated the analysis of von Blanckenburg et al. (2012), which compared $^{10}Be_{is}$-derived erosion rates and sediment yields to $^{10}Be_{met}/^{9}Be_{reactive}$-derived erosion rates using a mass balance

formulation (eq. 1). In agreement with the von Blanckenburg et al. (2012) analysis, I assumed $[^{9}Be]_{parent}$ was equal to the global crustal average ^{9}Be concentration of 2.5 ppm for all samples (Kabata-Pendias et al. 2011).

$$f.factor = \frac{F_{met}^{^{10}Be}}{[^{9}Be]_{parent} * D * \left(\frac{^{10}Be_{met}}{^{9}Be_{reactive}}\right)} \quad \text{(eq. 1)}$$

$$D = \frac{F_{met}^{^{10}Be}}{[^{9}Be]_{parent} * f.factor * \left(\frac{^{10}Be_{met}}{^{9}Be_{reactive}}\right)} \quad \text{(eq. 1')}$$

I calculated the fraction of ^{9}Be that has weathered out of bedrock or regolith, ($f_{reac}^{^{9}Be} + f_{diss}^{^{9}Be}$, termed $f.factor$ in this study) for each sample based on the flux of $^{10}Be_{met}$ in atoms/(mm^2*yr) ($F_{met}^{^{10}Be}$), a ^{9}Be concentration ($[^{9}Be]_{parent}$) of 1.67 *10^{17} atoms/g, $^{10}Be_{met}/^{9}Be_{reactive}$ measured in this study, and $^{10}Be_{is}$-derived erosion rates in mm/yr (D) (eq. 1). I then used the average $f.factor$ for each study area to calculate $^{10}Be_{met}/^{9}Be_{reactive}$,-derived erosion rates in mm/yr (D) from rearrangement of eq. 1. Erosion rates were converted to units of t/(km^2*yr) to match the units of von Blanckenburg et al. (2012).

3.0 Discussion of initial results

The following section discusses initial results for each hypothesis.

3.1 Method development (hypothesis 1)

Experiments performed to test potential $^{9}Be_{reactive}$ extraction methods indicate that leaching samples with 6M HCl for 24 hours in an ultrasonic bath extracts the entire grain coating (figure 1). The high precision of replicates (average deviation between replicates = 5%) suggests that the chosen method of HCl leaching reproducibly removes ^{9}Be from grain coatings. The Be

concentrations of standards measured approximately every ten samples indicate that ICP-OES detects Be concentrations consistently over time (figure 2). The coefficient of variation in the homogenized varve sediment samples that were extracted in triplicate with every batch of fluvial sediment samples was 9%. Overall, these results indicate that the reactive phase of ^{9}Be can be effectively and consistently leached from grain coatings using my HCl ^{9}Be extraction procedure and Be concentrations can be determined with ppb resolution using ICP-OES.

3.2 Statistical analyses of Be isotope data and watershed characteristics (hypothesis 2)

The significance of correlations between $^{10}Be_{is}$, $^{10}Be_{met}$, $^{9}Be_{reactive}$ and $^{10}Be_{is}$-derived erosion rates differs according to study location (figure 3; table 1). $^{10}Be_{met}$ and $^{9}Be_{reactive}$ significantly correlate ($R^2 > 0.5$, p value < 0.05) in 3 of the 7 watersheds sampled; $^{10}Be_{met}$ and $^{9}Be_{reactive}$ do not significantly correlate when considering all samples. The lack of significant co-variation between $^{10}Be_{met}$ and $^{9}Be_{reactive}$ in many study areas suggests that in some watersheds, ^{10}Be and $^{9}Be_{reactive}$ isotopes are not well mixed. If ^{9}Be atoms are concentrated deeper in the soil column and $^{10}Be_{met}$ concentrations are concentrated closer to the surface, deep erosion events would remove more $^{9}Be_{reactive}$ than shallow erosion. Watersheds with similar erosion rates but different erosion regimes could have very different $^{10}Be_{met}/^{9}Be_{reactive.}$ In this way, initial results suggest that caution must be taken in interpretation $^{10}Be_{met}/^{9}Be_{reactive}$ data, especially in small study areas that may not be in isotopic equilibrium.

Considering all samples, the correlation between $^{10}Be_{met}/^{9}Be_{reactive}$ and $^{10}Be_{is}$ ($R^2 = 0.58$, p value < 0.001) is stronger than the correlation between $^{10}Be_{met}$ and $^{10}Be_{is}$ ($R^2 = 0.40$, p value < 0.001), table 2. When considering correlations in each study area, $^{10}Be_{is}$ and $^{10}Be_{met}$ significantly correlate in 1 watershed (CH1xx) while $^{10}Be_{is}$ and $^{10}Be_{met}/^{9}Be_{reactive}$ significantly correlate in 2 watersheds (CH1xx and CHb). Generally, correlations are stronger when data span a wide range of $^{10}Be_{is}$, $^{10}Be_{met}$, and $^{9}Be_{reactive}$ concentrations. There are several factors that could contribute to

variability in $^{10}Be_{is}$, $^{10}Be_{met}$ and $^{9}Be_{reactive}$ correlations, including unquantified dust inputs of ^{9}Be, $^{10}Be_{is}$ and $^{10}Be_{met}$ (Graly et al. 2010), variation of ^{9}Be concentrations of parent bedrock or regolith (Veselý et al. 2002), and remobilization of $^{10}Be_{met}$ or $^{9}Be_{reactive}$ (Bacon et al. 2012).

Correlations between $^{10}Be_{met}/^{9}Be_{reactive}$ and $^{10}Be_{is}$ -derived erosion rates are not significant in individual sampling locations or across all samples (table 2). When $^{10}Be_{met}$ concentrations were normalized to $^{10}Be_{met}$ depositional flux, $^{10}Be_{met}/^{9}Be_{reactive}$ and $^{10}Be_{is}$ -derived erosion rates still do not significantly correlate across all samples ($R^2 < 0.2$).

Very few watershed characteristics significantly correlate to $^{10}Be_{is}$, $^{10}Be_{met}/^{9}Be_{reactive}$ or $^{10}Be_{is}$-derived erosion rates (table 3). The only strong and significant correlations observed when considering all samples are between total basin relief and $^{10}Be_{is}$-derived erosion rates ($R^2 = 0.55$, p value < 0.001) and mean basin slope and $^{10}Be_{is}$-derived erosion rates ($R^2 = 0.46$, p value < 0.001). These results suggest that although total basin relief and mean basin slope significantly correlate to $^{10}Be_{is}$-derived erosion rates in some watersheds, most watershed characteristics do not consistently influence $^{10}Be_{met}$, $^{9}Be_{reactive}$ or $^{10}Be_{is}$ concentrations.

All together, these findings do not support the hypothesis that statistically significant relationships exist between $^{10}Be_{met}$, $^{10}Be_{is}$, $^{9}Be_{reactive}$, and $^{10}Be_{is}$-derived erosion rates across a diverse range of environmental conditions and characteristics. Significant correlations between some variables exist when considering data with a wide range of $^{10}Be_{is}$ concentrations, but there are no consistently significant correlations between Be isotope data in individual study areas.

3.3 Correlations between $^{10}Be_{met}/^{9}Be$-derived erosion rates and $^{10}Be_{is}$-derived erosion rates (hypothesis 3)

I found that $^{10}Be_{is}$-derived erosion rates significantly correlate to $^{10}Be_{met}/^{9}Be_{reactive}$-derived erosion rates (figure 3), and that the calculated $f.factor$ spans a wide range values in each study location (figure 4). It is important to note that because the $^{10}Be_{is}$-derived erosion rate was used to

calculate the $f.factor$ and the $f.factor$ was used to predict $^{10}Be_{met}/^{9}Be_{reactive}$ -derived erosion rates, the two measures of erosion are expected to correlate. In order to determine $^{10}Be_{met}/^{9}Be$-derived erosion rates without including $^{10}Be_{is}$-derived erosion rates in the calculation, we need an alternative method of calculating the $f.factor$. Further, the assumption that the ^{9}Be concentration of bedrock or regolith ($[^{9}Be]_{parent}$) is 2.5 ppm for all samples oversimplifies these calculations. In my dataset, several samples had a $f.factor$ greater than 1, which indicates that $[^{9}Be]_{parent}$ is greater than 2.5 ppm. A method of estimating the $[^{9}Be]_{parent}$ concentration will also improve our ability to assess if $^{10}Be_{is}$-derived erosion rates significantly correlate to $^{10}Be_{met}/^{9}Be_{reactive}$ -derived erosion rates.

4.0 Future work

While we do not have bedrock or regolith samples from our study areas to measure $[^{9}Be]_{parent}$, we can approximate ^{9}Be concentrations of parent materials by measuring ^{9}Be concentrations of the fluvial sediment grains. Assuming that the fraction of ^{9}Be in the dissolved phase ($f_{diss}^{^{9}Be}$) is very small (Takahashi et al. 1998), dividing $^{9}Be_{reactive}$ by the ^{9}Be in sediment grains gives an estimate of the $f.factor$ for each fluvial sediment sample. In the coming months, I will dissolve the fluvial sediment samples in HF and H_2SO_4, determine the $f.factor$ for each sample, and re-calculate $^{10}Be_{met}/^{9}Be_{reactive}$-derived erosion rates using the new $f.factor$ dataset. This will help me resolve remaining questions regarding hypotheses 3. I also may have more $^{9}Be_{reactive}$ HCl extractions to add to my study and 20-40 $^{9}Be_{reactive}$ HCl extractions to run for collaborators. Finally, I need to write a manuscript for publication and defend my thesis.

5.0 Timeline

A timeline is attached as figure 6.

Citations.

Bacon, A. R., D. DeB. Richter, P. R. Bierman, and D. H. Rood. (2012). "Coupling meteoric ^{10}Be with pedogenic losses of ^{9}Be to improve soil residence time estimates on an ancient North American interfluve." Geology **40**(9): 847-850.

Balco, G., J.O. Stone, N. A. Lifton, and T.J. Dunai. (2008). "A quick and easily accessible means of calculating surface exposure ages or erosion rates from ^{10}Be and ^{26}Al measurements." Quaternary Geochronology **3**: 174-195.

Barg, E., D. Lal, M. J. Pavich, M. W. Caffee, J. R. Southon. (1997). "Beryllium geochemistry in soils; evaluation of ^{10}Be/ ^{9}Be ratios in authigenic minerals as a basis for age models." Chemical Geology **140**(3-4): 237-258.

Bierman, P. R. (1994). "Using in situ produced cosmogenic isotopes to estimate rates of landscape evolution; a review from the geomorphic perspective." Journal of Geophysical Research. B, Solid Earth and Planets **99**(7): 13885-13896.

Graly, J. A., P. R. Bierman, L. J. Reusser, and M. J. Pavich (2010). Meteoric ^{10}Be in soil profiles-A global meta-analysis. Geochimica et Cosmochimica Acta **74**:6814-6829.

Graly, J.A., L.J. Reusser, and P.R. Bierman. "Short and long-term delivery rates of meteoric ^{10}Be to terrestrial soils." Earth and Planetary Science. **302**: 329-336.

Kabata-Pendias, A. (2011). *Trace Elements in Soils and Plants*: Berlin, New York, Springer, 135
Kabata-Pendias, A. and V. Szteke, (2015). "Trace Elements in Abiotic and Biotic Environments." 1st ed. Florida, Taylor & Francis Group, LLC: 29-33.

Lal, D. (1988). "In situ-produced cosmogenic isotopes in terrestrial rocks." Annual Reviews of Earth and Planetary Science. **16**: 355-388

Monaghan, M. C., S. Krishnaswami, and K. K. Turekian. (1986). "The global-average production rate of ^{10}Be." Earth and Planetary Science Letters **76**: 279-287.

Nichols, K.K., P.R. Bierman, and D.H. Rood. (2014). "^{10}Be constrains the sediment sources and sediment yields to the Great Barrier Reef from the tropical Barron River catchment, Queensland, Australia." Geomorphology **224:** 102-110.

Pavich, M. P., L. Brown, J. Klein, and R. Middleton (1984). "^{10}Be accumulation in a soil chronosequence." Earth and Planetary Science Letters **68**: 198-204.

Portenga, E. W. and P.R. Bierman. (2011). "Understanding Earth's eroding surface with ^{10}Be." GSA Today. **21**(8): 4-10.

Takahashi M., S. Ambe, Y. Makide, and F. Ambe (1998). "Comparison of adsorption behavior of multiple inorganic ions on kaolinite and silica in the presence of humic acid using the multi-tracer technique." Geochimica et Cosmochimica Acta. **63**: 815-836.

Trodick, C. D. (2011). *In situ and meteoric ^{10}Be concentrations of fluvial sediment collected from the Potomac River Basin.* Diss. University of Vermont, 2011. Burlington: Vermont.

Veselý J, S. A. Norton, P. Skřivan, V. Majer, P. Krám, T. Navrátil and J M Kaste (2002). "Environmental Chemistry of Beryllium. In Beryllium: mineralogy, petrology, and geochemistry." Reviews in Mineralogy and Geochemistry. **50**: 291-317.

Von Blanckenburg, F., J. Bouvchez, and H. Wittmann. (2012). "Earth surface erosion and weathering from the ^{10}Be (meteoric)/^{9}Be ratio." Earth and Planetary Science Letters **351:** 295-305.

location	climate	tectonic setting	Rock type/parent material	MAP (mm/yr)	Sample ID	N
Potomac River (eastern United States)	humid, temperate, never glaciated	passive margin	metamorphic rocks, sandstone, shale, and carbonate	700-1000	POT	62
Barron River (NE Australia)	humid, temperate, never glaciated	passive margin	granite and biogenetic carbonate	1900-2200	GLD	14
Georges River (SE Australia)	humid, temperate, never glaciated	passive margin	sandstone, granodiorite	900-1200	G	8
Mekong River (SE China)	tropical, never glaciated	tectonically active	lightly metamorphosed granite and sedimentary red beds	900-1600	CH1xx CHa CHb CHc	64 15 24 15

Table 1. Climate and geologic background for fluvial sediment samples analyzed in this study.

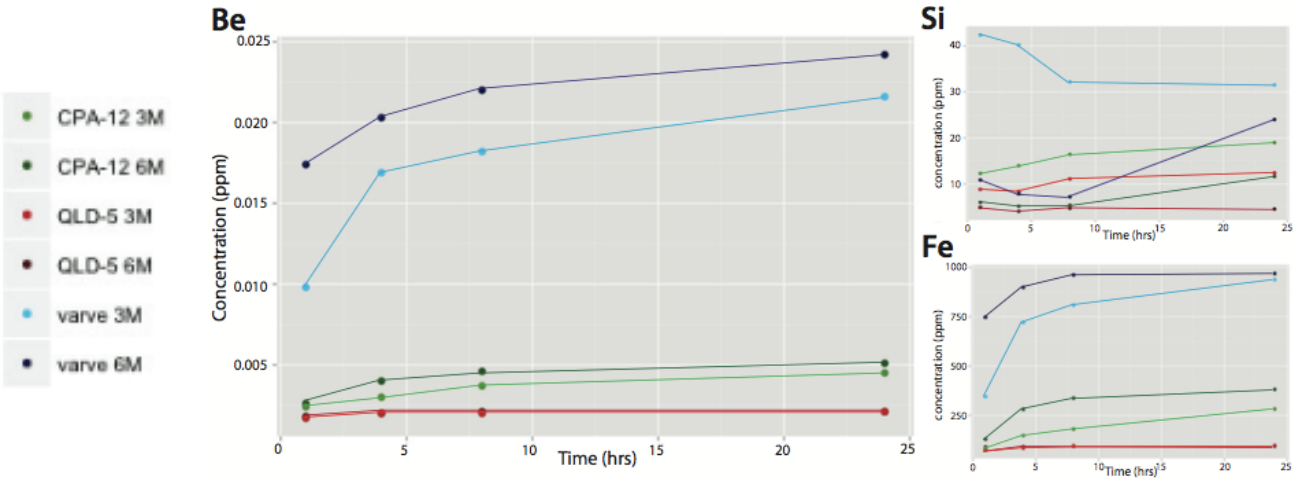

Figure 1. Soil samples (CPA-12), fluvial sediment samples (QLD-5) and glacial lake sediment samples (varve) were extracted with 3M or 6M HCl for 1, 3, 8 and 24 hours in an ultrasonic bath. Concentrations of Be (detected at 313.107 nm), Fe (271.441 nm) and Si (231.611 nm) measured with ICP-OES after 24 hours of reaction time indicate that the dissolution of grain coatings plateaus. Dissolved Si concentrations are low, indicating that HCl does not attack primary silicates.

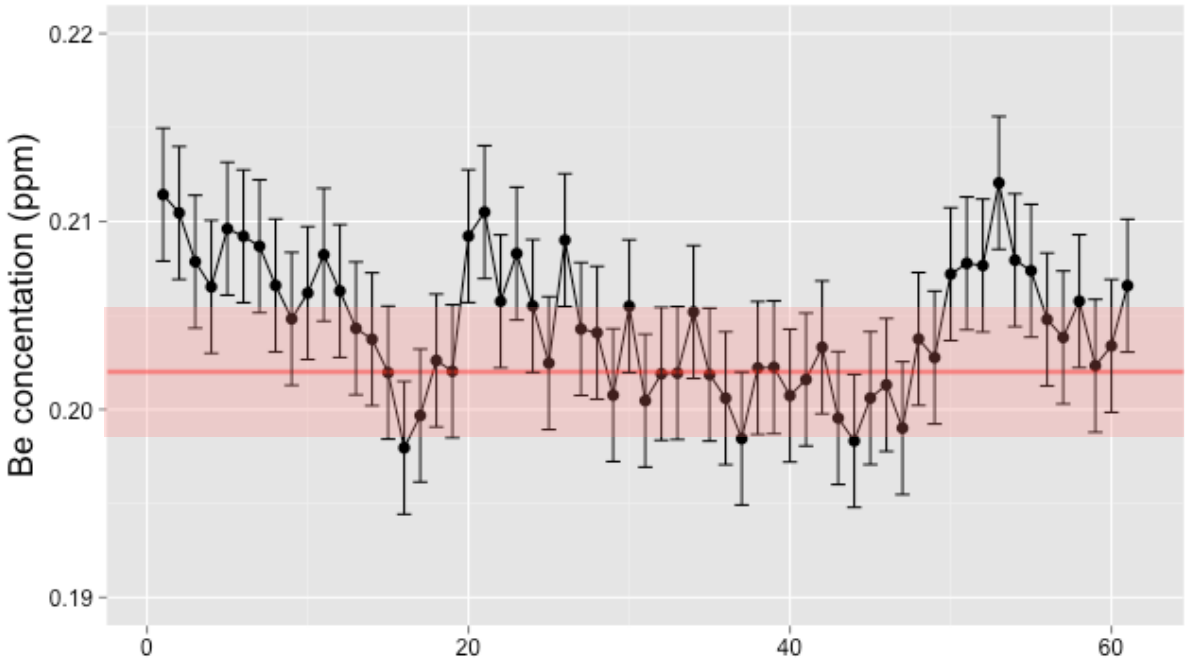

Figure 2. Be concentration of lab standards with elemental concentrations similar to sample leachates were measured every ~10 samples during ICP-OES runs. Red line represents the gravimetrically calculated Be concentration of the standard, red bars represents 1 SD above and below calculated concentration, error bars on each point represent 1SD above and below the measured concentration.

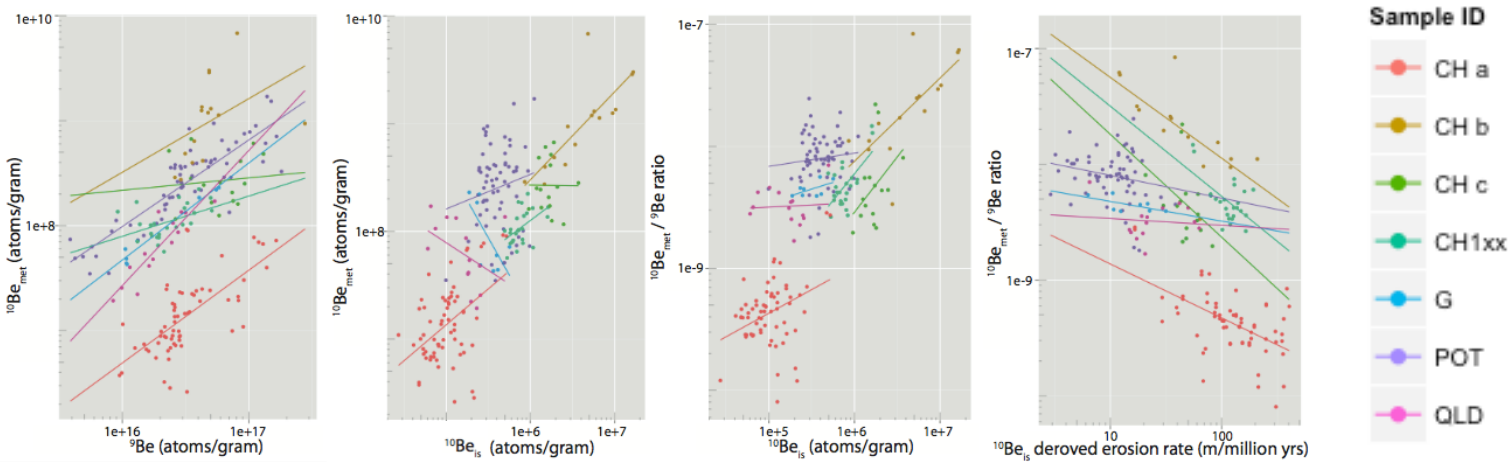

Figure 3. Plots of Be isotope data and $^{10}Be_{is}$-derived erosion rates with linear regression lines for each study area. Correlations between $^{10}Be_{is}$ and $^{10}Be_{met}$ and correlations between $^{10}Be_{met}/^{9}Be_{reactive}$ and $^{10}Be_{is}$ are significant across a wide range of $^{10}Be_{is}$ concentrations, but are not always significant when considering individual study areas with a smaller range of concentrations (table 2).

		$^{9}Be_{reactive}$ vs $^{10}Be_{met}$		$^{10}Be_{is}$ vs $^{10}Be_{met}/^{9}Be_{reactive}$		$^{10}Be_{is}$ vs $^{10}Be_{met}$		Erosion rate vs $^{10}Be_{met}/^{9}Be_{reactive}$	
Study Region	**N**	**R^2**	**p-value**	**R^2**	**p-value**	**R^2**	**p-value**	**R^2**	**p-value**
POT	62	**0.5**	**<0.001**	8E-04	0.83	0.07	0.05	0.03	0.18
QLD	14	**0.75**	**<0.001**	0.19	0.12	0.03	0.58	0.0036	0.84
G	8	**0.99**	**<0.001**	0.36	0.12	0.45	0.07	0.33	0.14
CH1xx	64	**0.39**	**<0.001**	**0.53**	**<0.001**	**0.52**	**<0.001**	0.13	0.003
CHa	15	0.01	0.73	**0.45**	**0.006**	0.18	0.12	0.28	0.041
CHb	24	**0.31**	**0.005**	**0.63**	**<.001**	0.19	0.03	0.27	0.009
CHc	15	0.031	0.53	0.048	0.43	0.002	0.88	0.09	0.28
All Samples	202	0.084	<0.001	**0.58**	**<0.001**	**0.4**	**<0.001**	0.11	<0.001

Table 2. Coefficient of determination (R^2) and p values for correlations between Be isotope dataset in individual study areas and across all samples. Pink type represents correlations with a p value less than 0.05 and an R^2 greater than 0.5. Blue type represents correlations with a p value less than 0.05 and a R^2 greater than 0.3.

	N	watershed characteristic	$^{10}Be_{is}$		$^{10}Be_{met}/^{9}Be_{reactive}$		$^{10}Be_{is}$-erosion rate	
			R^2	p-value	R^2	p-value	R^2	p-value
POT	62	MAP	0.03	0.21	0.01	0.56	0.12	0.005
		mean basin slope	0.001	0.86	0.03	0.17	0.06	0.05
		total relief	<0.001	0.96	0.05	0.07	0.01	0.44
QLD	14	MAP	0.09	0.31	**0.36**	**0.02**	0.27	0.06
		mean basin slope	0.06	0.41	0.20	0.11	**0.53**	**0.003**
		total relief	0.03	0.55	0.01	0.72	<.001	0.95
G	8	MAP	**0.91**	**<0.001**	**0.59**	**0.02**	**0.77**	**0.004**
		mean basin slope	0.4	0.09	0.07	0.52	0.09	0.47
		total relief	0.13	0.38	0.28	0.18	0.03	0.68
CH1xx	64	MAP	0.01	0.44	0.03	0.21	0.24	<0.001
		mean basin slope	0.02	0.25	0.02	0.22	0.12	0.004
		total relief	0.01	0.36	0.10	0.01	0.26	<.001
CHa	15	MAP	**0.69**	**<0.001**	**0.30**	**0.04**	**0.43**	**0.008**
		mean basin slope	**0.78**	**<0.001**	0.17	0.12	**0.39**	**0.01**
		total relief	0.29	0.03	0.26	0.05	0.1	0.25
CHb	24	MAP	0.34	0.003	0.16	0.06	0.29	0.006
		mean basin slope	0.08	0.18	0.01	0.06	0.22	0.02
		total relief	0.04	0.002	0.37	0.002	0.21	0.03
CHc	15	MAP	0.05	0.41	**0.33**	**0.03**	0.10	0.26
		mean basin slope	0.33	0.02	**0.06**	**0.001**	0.22	0.08
		total relief	<.001	0.93	0.04	0.48	0.003	0.85
All Samples	202	MAP	0.002	0.53	0.03	0.01	0.009	0.18
		mean basin slope	0.003	0.46	0.03	0.01	**0.46**	**<0.001**
		total relief	0.02	0.03	0.11	<0.001	**0.55**	**<0.001**

Table 3. Coefficient of determination (R^2) and p values for correlations between Be isotope data and watershed characteristics in individual study areas and across all samples. Pink type represents correlations with a p value less than 0.05 and an R^2 greater than 0.5. Blue type represents correlations with a p value less than 0.05 and a R^2 greater than 0.3.

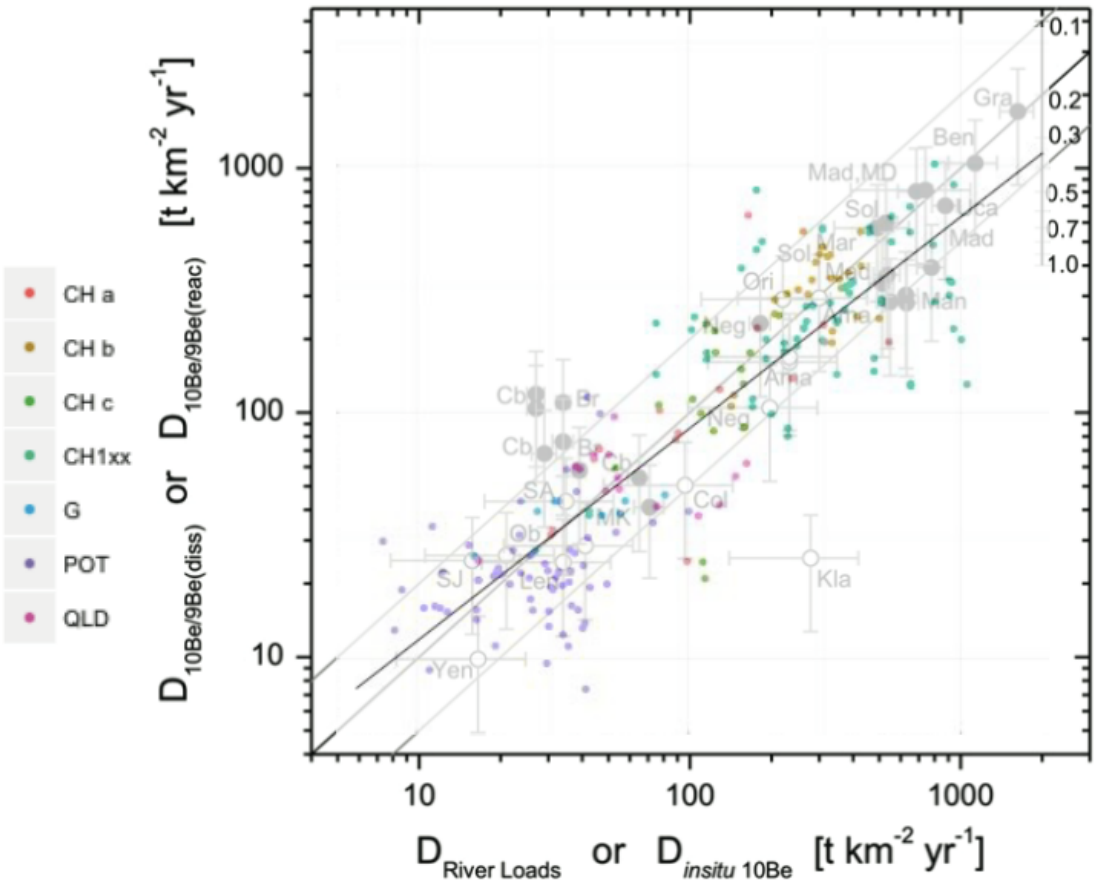

Figure 4. Data from this study (in color) are overlaid on figure from von Blanckenburg et al. (2012) (greyscale). Von Blanckenburg et al. (2012) data includes denudation rates calculated from sediment loads and $^{10}Be_{is}$; the center black line represents the linear least squares regression fit. Data from my study only includes $^{10}Be_{is}$-derived erosion rates; black line represents the linear least squares regression line for all samples. Black numbers in top right represent the y intercept of lines with a constant f.factor (0.1 through 1.0). Both datasets show a significant correlation between $^{10}Be_{is}$-derived erosion rates and $^{10}Be_{met}/^{9}Be_{reactive}$-derived erosion rates.

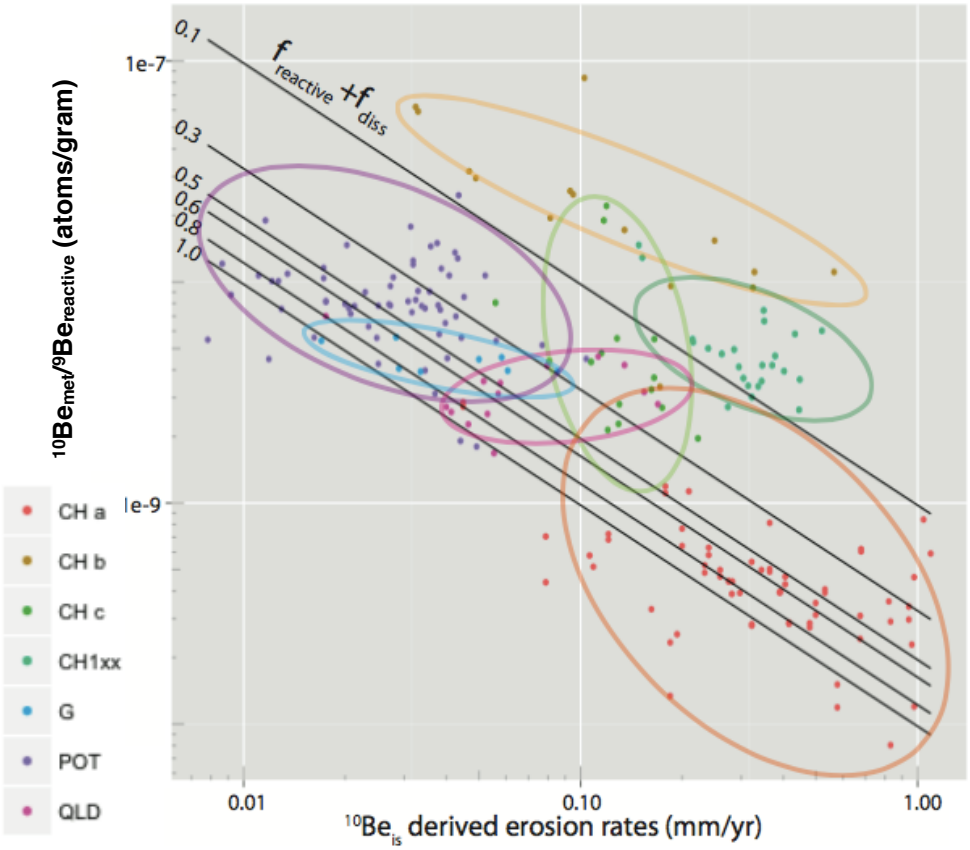

Figure 5. Comparison of $^{10}Be_{met}/^{9}Be_{reactive}$ and $^{10}Be_{is}$-derived erosion rates; lines represent f.factors ($f_{reactive}$ + $f_{dissolved}$) between 0.1 and 1, calculated using the average $^{10}Be_{met}$ flux for all data and an assumed $^{9}Be_{parent}$ concentration of 2.5 ppm. Data span a wide range of f.factors, and are grouped by study area. Some data appear to have an f.factor greater than 1, which implies a ^{9}Be concentration higher than 2.5 ppm.

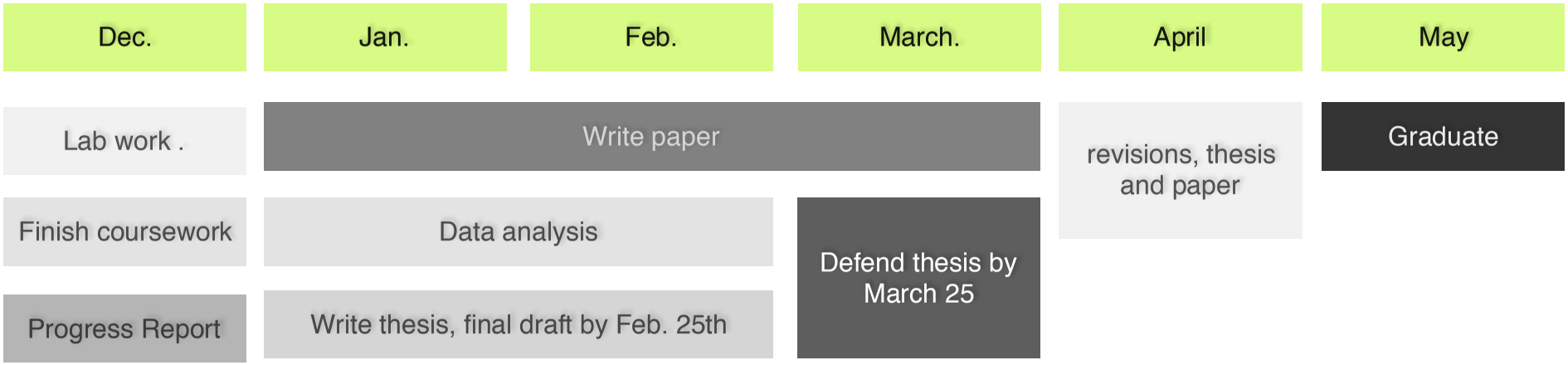

Figure 6. Timeline for completion of masters degree.

Appendix 1.

I optimized the ICP-OES method by selecting the most sensitive emission lines, adjusting the amount of time the instrument measures sample (integration time), the speed that it pumps new sample before it begins measurements (transfer time), and the rinse time between samples (rinse time). Be was the only element measured on the monochromator; I changed the monochromator settings to the highest possible sensitivity and precision (table 1).

After taking scans of all of the measured emission lines, I also adjusted the locations that the instrument took background measurements (reported in nm to the right and the left of the predicted emission peak) to better reflect baseline signal (table 2). In order to correct for non-linear calibration curves, I fit my curves with a two variable polynomial function that weighted the calibration parameters according to a formula that minimized error in the range of concentrations I expected to have the most samples. For example, the Be standard curve was slightly nonlinear in the highest concentration standard, so I fit the calibration curve with a polynomial that weighted the lower concentration standards more than the highest concentration. This ensured that the lowest Be measurements (1-10 ppb) had the least error possible (we had very few samples with concentrations near the highest calibration standard). The calibration weighting formulas and all other calibration parameters are listed in table 2.

	time (s)	pump speed
Rinse	10	normal
Transfer	40	high speed
Integration	0.5	fast

mono line specifications	
Sensitivity	high
rapid-precise	very precise

Table 1. Acquisition parameters for “SgHClLeach61815” method used for analysis of fluvial sediment samples.

Appendix 1.

poly/ mono	element	line (nm)	calibration weighting formulas (c = concentration)	Left background (nm)	Right background (nm)	number of variables in polynomial calibration curve fit
poly	Al	309.271	1/c	0.075	0.069	2
mono	Be	313.107	1/sqrt(c)		0.018	2
poly	Ca	313.997	1/c	0.096	0.096	2
poly	Fe	271.441	1/c	0.03	0.036	2
poly	K	766.49	$1/c^2$	0.036	0.024	2
poly	Mg	279.079	1/sqrt(c)	0.036		2
poly	Mn	259.373	1/sqrt(c)	0.05	0.05	2
poly	Na	589.592	1/sqrt(c)	0.05	0.05	2
poly	Si	251.611	1/sqrt(c)	0.02	0.02	2
poly	Ti	334.94	$1/c^2$	0.05	0.05	2

Table 2. Calibration parameters and background settings for “SgHClLeach61815” method used for analysis of fluvial sediment samples.